FISEVIER

Contents lists available at ScienceDirect

Journal of Colloid and Interface Science

journal homepage: www.elsevier.com/locate/jcis



Regular Article

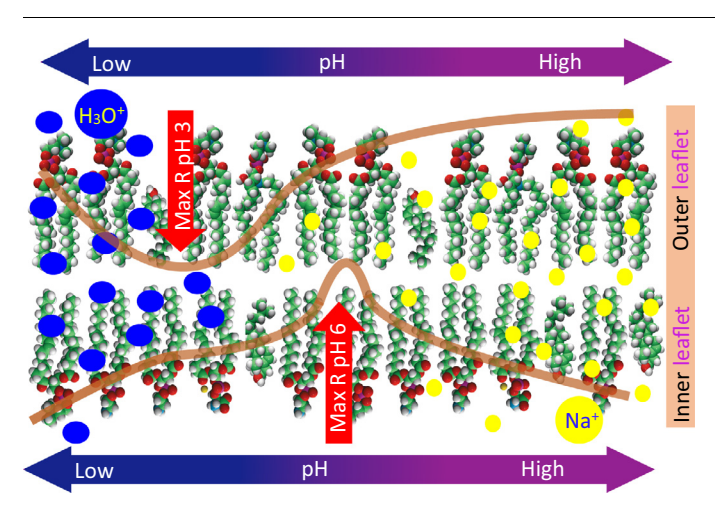
pH dependent electrical properties of the inner- and outer- leaflets of biomimetic cell membranes



Vitalii I. Silin ^{a,*}, David P. Hoogerheide ^b

- ^a University of Maryland, Institute for Bioscience and Biotechnology Research, Rockville MD 20850, USA
- ^b Center for Neutron Research, National Institute of Standards and Technology, Gaithersburg, MD 20899, USA

G R A P H I C A L A B S T R A C T



ARTICLE INFO

Article history: Received 15 October 2020 Revised 16 February 2021 Accepted 3 March 2021 Available online 10 March 2021

Keywords:
Biomembranes
EIS
SPR
Neutron reflectometry
Phospholipid interactions
pH

ABSTRACT

Composition and asymmetry of lipid membranes provide a means for regulation of *trans*-membrane permeability of ions and small molecules. The pH dependence of these processes plays an important role in the functioning and survival of cells. In this work, we study the pH dependence of membrane electrical resistance and capacitance using electrochemical impedance spectroscopy (EIS), surface plasmon resonance (SPR) and neutron reflectometry (NR) measurements of biomimetic tethered bilayer lipid membranes (tBLMs). tBLMs were prepared with single-component phospholipid compositions, as well as mixtures of phospholipids (phosphatidylcholine, phosphatidylserine, phosphatidylethanolamine, sphingomyelin and cholesterol) that mimic the inner- and outer- leaflets of plasma cell membranes. We found that all studied tBLMs have a resistance maximum at pHs near the pK_a s of the phospholipids. SPR and NR indicated that surface concentration of phospholipids and the thickness of the hydrophobic part of the membrane did not change versus pH. We postulate that these maxima are the result of protonation of the phosphate oxygen of the phospholipids and that hydronium ions play a major role in the conductance at pHs < pK_a s while sodium ions play the major role at pHs > pK_a s. An additional sharp resistance maximum of the PE tBLMs found at pH 5.9 and most likely represents the phosphatidylethanolamine's isoelectric point. The data

Abbreviations: SPR, surface plasmon resonance; EIS, electrochemical impedance spectroscopy; PL, phospholipids; tBLM, tethered bilayer lipids membrane; NR, neutron reflectometry; PC, 1-palmitoyl-2-oleoyl-sn-glycero-3-phospho-(1'-rac-glycero) (sodium salt); PS, 1-palmitoyl-2-oleoyl-sn-glycero-3-phospho-i-serine (sodium salt); PE, 1-palmitoyl-2-oleoyl-sn-glycero-3-phosphoethanolamine; DOTAP, 1,2-dioleoyl-3-trimethylammonium-propane (chloride salt); SM, N-palmitoyloleoyl-p-erythro-sphingosylphosphorylcholine; ePC, 1-O-hexadecanyl-2-O-(9Z-octadecenyl)-sn-glycero-3-phosphocholine; Chol, cholesterol.

* Corresponding author.

E-mail address: vsilin@umd.edu (V.I. Silin).

show the key roles of the characteristic parts of phospholipid molecules: terminal group (choline, carboxyl, amine), phosphate, glycerol and ester oxygens on the permeability and selectivity of ions through the membrane. The interactions between these groups lead to significant differences in the electrical properties of biomimetic models of inner- and outer- leaflets of the plasma cell membranes.

© 2021 Elsevier Inc. All rights reserved.

1. Introduction

Lipids form a mechanical, biochemical and electrical barrier between the cells and the main compartments inside the cell. Lipids provide the means for signal transduction, serve as energy storage and as secondary messengers [1-2]. They can also play a role as cofactors to modulate protein activity [3]. More than 40,000 naturally occurring lipids have been found with modern lipidomics tools to fulfill the multi-faceted functions of the membrane [4], and many physical chemical properties of lipids in the membranes of living cells are well understood [1,5]. The membrane's lipid composition defines its structure, as well as its interactions with ions, proteins, peptides, and other biomolecules. The lipid composition and pH play the major role in vesicle trafficking inside the cell and in the processes of endocytosis and exocytosis during viral infections [6]. Direct fusion of SARS corona viruses [7] with the cell membranes or endosome-assisted endocytosis of flaviviruses [8] depend on PL composition and pH.

In general, membranes are nonconductive and maintain electrical potential [2] by creating a barrier to electrolytes. However, background membrane currents are known to provide an additional function [2] of transporting ions and small molecules through this barrier. Specific ion transport depends on the structure and the dynamics, the composition, the asymmetry of the bilayer, the nature and concentration of the electrolyte ions, and on the pH [2], which can range [9–10] from 4 to 8 for most cells; although the pH outside of the bacterial cell membranes [11] can range from 1 for acidophiles [12] to 9 for alkaliphilic [13] bacteria.

pH plays an important role in membrane function [14–15]. In general, the influence of pH on the hydrogen bonding, the charge of the lipids head groups and phase transition temperatures is known [1]; however, there is little experimental work that systematically studies the dependence of membrane electrical properties [16–23] on pH. In many cases, when studying membrane-protein or -peptide interactions, the influence of pH and lipid composition on the properties of the membrane is not taken into account, although the influence of pH and PL composition on mechanical

and electrical properties [24] and on the many membrane processes must be taken in consideration [2].

One of the major lipid components of cell membranes are glycerophospholipids [5] (PLs). Phosphatidylcholines, phosphatidylethanolamines, phosphatidylserines, together with sphingomyelin and cholesterol, are the main (accounting for more than 90% of all lipids) building blocks of the plasma membranes [3]. The distribution of these PLs in the inner and outer membrane leaflets is asymmetrical [12]: phosphatidylethanolamine and phosphatidylserine are enriched in the inner leaflet, phosphatidylcholine and sphingomyelin in the outer. Cholesterol is generally found to be distributed in both leaflets [25]. The asymmetry of leaflet composition has important biological functions, however studies of these membranes are limited mostly due to experimental difficulties [1,5,26].

In this work, the effect of pH and the composition of PLs on the electrical resistance and the capacitance of biomimetic planar phospholipid membranes, so called tethered bilayer lipid membranes (tBLMs), are examined. The PL compositions in the tBLMs mimic the steady state compositions of the inner- and outer- leaflets of plasma membranes [3]. To limit the number of variables in the experiments and to isolate the impact of the head groups of phospholipids, we use PLs with aliphatic chain lengths of 16:0–18:1 (Fig. 1); we also keep the temperature and concentration of salt ions constant. We employ an experimental platform that was developed in our lab for tBLMs: simultaneous surface plasmon resonance (SPR) and electrochemical impedance spectroscopy (EIS) measurements [see Fig. S1–Fig. 3S supplemental material section].

2. Experimental section

2.1. Reagents for tBLM preparations

Powders of the lipids (purity > 99%) 1-palmitoyl-2-oleoyl-*sn-glycero*-3-phosphocholine (PC), 1-palmitoyl-2-oleoyl-*sn-glycero*-3-phospho-(1'-*rac*-glycerol) (sodium salt) (PG), 1-palmitoyl-2-

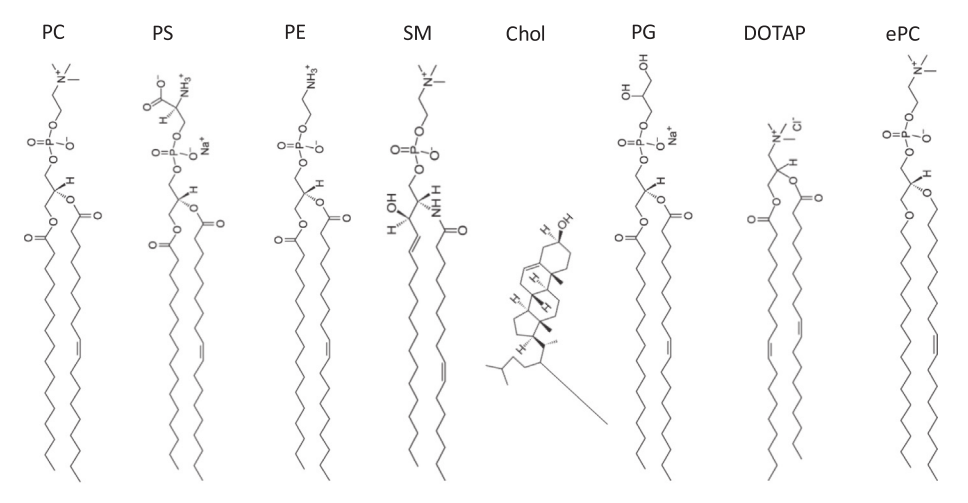


Fig. 1. Lipids used to form biomimetic tBLMs.

Table 1Buffers used for pH adjustment.

Buffers, 50 mM	pH range
Glycine	1.74-3.24
Acetate	3.75-5.35
HEPES	5.72-6.6
MES	6.83-8.02
Glycine	8.56-10

oleoyl-sn-glycero-3-phospho-L-serine (sodium salt) (PS), 1palmitoyl-2-oleoyl-sn-glycero-3-phosphoethanolamine (PE), 1,2-d ioleoyl-3-trimethylammonium-propane (chloride salt) (DOTAP), N-palmitoyloleoyl-p-erythro-sphingosylphosphorylcholine (SM), an ether PC: 1-O-hexadecanyl-2-O-(9Z-octadecenyl)-sn-glycero-3phosphocholine (ePC) and cholesterol (Chol) were purchased from Avanti Polar Lipids (Alabaster, AL) and dissolved in anhydrous ethanol (purity > 99.5%) (Sigma-Aldrich, St. Louis, MO) or, if not soluble in ethanol, in distilled chloroform (purity > 99.5%) (Sigma-Aldrich, St. Louis, MO), to a final concentration of 10 mM (M = mol/L). Mixtures of PLs were prepared in chloroform. A lipid thiol lipid mimic 1,2-di-O-myristyl-3-[ω-mercaptohexa(ethylene oxide) glycerol (WC14), synthesized and purified (purity > 99%) in our laboratory [27], was used as a tethering molecule to form the tBLMs on gold surfaces. 2-Mercaptoethanol (β ME) (purity > 99%) (Sigma-Aldrich, St. Louis, MO) was used as a space-filling component between WC14 molecules and was distilled before use. Buffers (50 mM) used are shown in Table 1 all contained sodium chloride (150 mM) (purity > 99.5%). Glycine (purity > 99%), acetic acid and sodium acetate (purity > 99%), 4-(2-Hydroxyethyl)pipera zine-1-ethanesulfonic acid (HEPES) (purity > 99.5%), 2-(Nmorpholino)ethanesulfonic acid (MES) (purity > 99.5%) were purchased form Sigma Aldrich St. Louis, MO. For buffer preparation, purified water with resistance 18.2 M Ω /cm was used.

2.2. SPR/EIS setup and tethered bilayer lipid membrane formation

Fig. 1S-Fig. 3S SPR/EIS measurements were conducted with a home-built SPR instrument combined with an electrochemical impedance spectroscopy station (Solartron Analytical, Farnborough, U.K.), using a saturated silver – silver chloride MI-401F reference electrode (Microelectrodes, Inc., Bedford, NH). EIS measurements were taken at 0 potential. The details on the SPR/EIS measurements system, SPR calibration for thickness measurements and EIS data collection and analysis have been previously described [28].

Detailed procedures for tBLM formation on gold has been described previously [28]. Briefly, the SPR/EIS chips comprise sapphire substrates (Rubicon Technology, Inc., Bensenville, IL) that are coated by magnetron sputtering on a Denton Vacuum Discovery 550 Sputtering System at the NIST Center for Nanoscale Science and Technology cleanroom Gaithersburg, MD USA with 0.5 nm chromium and 46 nm gold films, then incubated overnight in a 0.2~mM ethanol solution of WC14/ β ME (20/80 M ratio) to form a mixed self-assembled monolayer (SAM) of WC14/BME. After rinsing with ethanol and drying in nitrogen stream, the SAM-coated chip was installed in the SPR/EIS cell [(1 mL volume) equipped with a perfluoro elastomer Kalrez O-ring (i.d. = 6 mm)]. A tBLM was formed with the fast solvent exchange method [29] using a buffer at pH 7.5. To form the tBLM, 40 µL of a PL solution was injected into the SPR/EIS cell with the SAM-coated chip, incubated for 2 min, and then rigorously washed with 100 mL of HEPES buffer at pH 7.5. Overlayers of PL molecules were removed from the tBLM by incubation in a 10% to 20% ethanol solution in water for 10 min (Fig. 4S). Fig. 2S C shows the characteristic small semicircle in Cole-Cole plots of the EIS spectra of a fully-formed tBLM in comparison

with EIS spectra that do not have a tBLM (large gray line semicircle in Fig. 2S C). Because EIS is not very sensitive to overlayers, the changes in this small semicircle were monitored during the washing to remove overlayers in order to prevent thinning of the tBLM.

The absolute values of capacitance and resistance of tBLMs depend strongly on the surface density of tethering molecules at the surface. We chose the lowest molar ratio (20/80) of WC14/ β ME for tBLM formation that provided stable membranes for the duration of our experiments to minimize the influence of tethering molecules on the structure of the proximal (to the gold) leaflet of the tBLM, ensuring that proximal and distal leaflets have maximum compositional symmetry.

To change buffers in the cell, 950 µL of the buffer was taken from the cell (50 μ L was left to keep the tBLM intact) and was replaced with 950 μL of the new buffer. This procedure was repeated 5 times. As shown in Fig. 5S A, immediately after the buffer was replaced with a different pH, the resistivity of the bilayer changed and only stabilized after approximately 60 min. Moreover, as shown in Fig. 5S B, there is significant hysteresis when changing pH. Thus, for consistency, measurements were conducted after changing the pH incrementally (0.5 units) in one direction. After tBLM preparation at pH 7.5, buffer was changed to pH 3 and the tBLM was incubated overnight. Measurements started at the lowest pH (pH = 2) after incubation (~30 min) or until the resistance stabilized. During tBLM incubation in a particular buffer (Table 1), EIS measurements were conducted every 2–3 min for 10–15 min or until the resistance of the membrane did not change (<7-10%). After the completion of the measurements (pH = 10), the pH was returned to 3, incubated overnight, and EIS data obtained to confirm tBLM stability. Examples of EIS data and the fit to the equivalent circuit model (shown in the Fig. 1S) to obtain the resistance (R_m) and the capacitance (C_m) of the tBLMs at different pHs are shown in Fig. 2S.

SPR measurements (Fig. 3S), conducted every 2 s for the duration of the experiment, were used for tBLM thickness measurements and to ensure that the tBLM was stable after buffer substitutions. The changes in the SPR signal for different buffers (Fig. 3S) is due to the differences in the buffer bulk refractive index. After the completion of each experiment, SPR was used to measure the tBLM thickness. For this, the SPR/EIS chip was washed with ethanol or chloroform and the difference in SPR response before and after the wash indicated the amount of the PL in the tBLM. To ensure complete PL removal the buffer was initially replaced with water, then the cell was rinsed with ethanol (5 mL for 5 min), followed by a water wash, (10 mL) and, finally, the last buffer (Fig. 6S A). For PLs soluble in chloroform two additional steps were used: ethanol rinse followed with chloroform rinse for 5 min, then back: with ethanol, water and buffer. An additional control for PL removal was provided by the EIS measurement of the sample surface (Fig. 6S B) which insured that the EIS signal was identical to the EIS spectra on the surface of the chip that was not used for tBLM preparation.

Reproducibility of the tBLM formation and thickness measurements was 8% as measured at four independently formed PC tBLMs. All measurements were conducted at 25.0 \pm 0.3 °C.

2.3. Sample preparation for neutron reflectometry

Silicon wafers (100, n-doped to a conductivity of 1–100 Ω cm) of 5 mm thickness and 75 mm diameter were coated with 40 Å Cr followed by 140 Å Au by magnetron sputtering, just as for the SPR/EIS samples. The substrate was then immersed for 8 h in an ethanolic solution of the thiol-lipid linking molecule [30] WC14 and β ME in a 3:7 M ratio and a total concentration of 0.2 mM. The resulting SAM was rinsed in ethanol and dried in a nitrogen stream. The coated surface of the sample wafer was mounted facing a 100 μ m

reservoir defined by a 65-mm inner diameter cylindrical Viton gasket separating the sample wafer from a rough backing wafer. The backing wafer was perforated by single inlets and outlets, which were coupled by flat-bottomed fittings (IDEX Health and Science Oak Harbor, WA) to external tubing for solution exchanges, which were performed using at least 7.5 mL flowing at 2.5 mL/min. A 10 mg/mL solution of PG was prepared in a pH 3 buffer and subjected to bath sonication for 40 min, at which time the solution was translucent. The lipid solution was injected into the flow cell and allowed to incubate for 1.5 h before rinsing with a heavy water (purity > 99.5%) (Sigma-Aldrich, St. Louis, MO) solution of 150 mM NaCl buffered to pD 1.95 with 25 mM glycine.

2.4. Neutron reflectometry

NR experiments were carried out on the NG7 horizontal reflectometer at the National Institute for Standards and Technology (NIST) Center for Neutron Research (NCNR). A monochromatic beam of wavelength $\lambda=4.768 \mbox{\normalfont A}$ impinged on the interface between the coated surface of the sample wafer and the liquid in the reservoir. The pre-sample collimating slits were chosen to maintain a constant illuminated interface area for each measured angle θ . The post-sample collimation was chosen to allow the entire reflected beam to impinge on the detector, which was positioned at an angle 2θ relative to the incoming beam direction to measure specular reflection. Each reflectivity curve covered a range in scattering wavevector $Q_z=4\pi\lambda^{-1} sin(\theta)$ from 0.008 Å $^{-1}$ to 0.239 Å.

The reflectivity was calculated as $R=(I(Q_z)-I_B(Q_z))/I_0(Q_z)$. Here $I(Q_z)$ is the measured count rate (normalized to a much larger monitor count rate to account for fluctuations in beam intensity). $I_B(Q_z)$ is the background intensity, which arises primarily from incoherent scattering from the liquid reservoir and is calculated by linear interpretation of the scattering intensity measured by rotating the sample to $\pm \Delta \theta = \pm (2Q_z + 0.15)$, for θ in degrees and Q_z in Å⁻¹, relative to the specular condition. $I_0(Q_z)$ is the incident beam intensity and is directly measured through the silicon

substrate at $\theta = 0$ with the detector positioned in line with the incident beam.

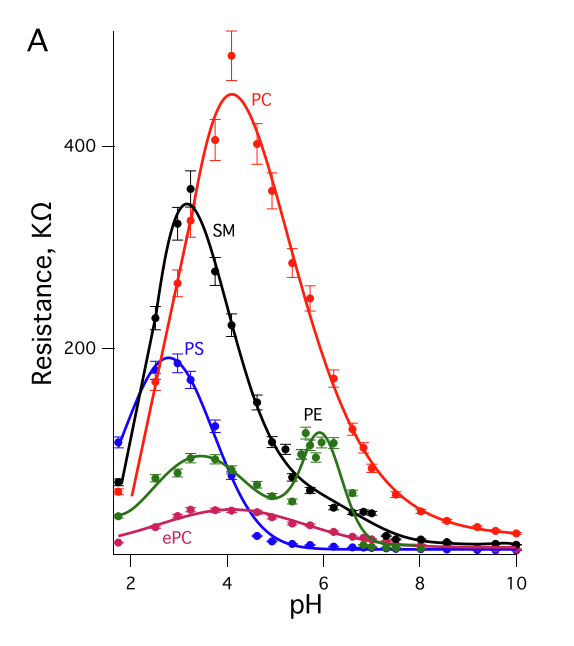
2.5. Composition space modeling

For each sample condition, the reflectivity was measured in both D₂O and H₂O-based buffers. Use of two "solvent contrasts" allow the physical parameters of the sparsely tethered bilayer to be precisely determined, as described elsewhere [31]. NR data were modeled using the composition space modeling procedures described previously for supported lipid bilayers [32]. Because all data were collected on the same physical substrate, all models were optimized with shared parameters for the substrate; only membrane-defining parameters such as surface-membrane separation and hydrophobic thickness were allowed to vary for individual bilayers. Optimizations were performed on the Bridges [33–34] high performance computing system using the DREAM Markov Chain Monte Carlo (MCMC) algorithm [35] implemented in the software package Refl1D [36]. Confidence intervals (CI) on parameters and model predictions were calculated from parameter distributions derived from at least 2.4 million DREAM samples after the optimizer had reached steady state.

3. Results and discussion

3.1. Single component membranes

Electrical resistance depends on the type of ions, ion concentration, and the mechanism of ion transport through the membrane [1]. Fig. 2A and B shows the dependence of the electrical resistance and capacitance on pH for single component PL tBLMs. The data show that all tBLMs have the smallest resistance at the highest and the lowest pHs and have maximum resistances at pHs between 3 and 4 (Table 2). PE has an additional maximum at 5.9 and will be discussed subsequently. The values of the resistance R_m versus pH differ significantly (for example, more than 10 times for PC and ePC tBLMs) for tBLMs over this set of phospholipid molecules (Fig. 2 A and Table 2). The capacitance C_m shows a



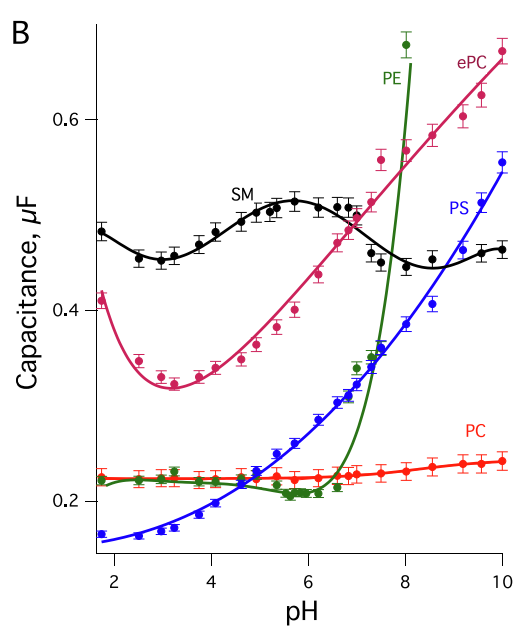


Fig. 2. Dependence on pH of (A) resistance and (B) capacitance of tBLMs prepared using individual PLs. Error bars were estimated from the covariance matrix derived from the optimization of the circuit equivalent model (Fig. 1S) to 51 impedance data points using a Levenberg Marquardt algorithm. Points are experimental data, lines –guide the eye.

Table 2 pH_{max} at resistance maxima R_{max} , pK_a values of PLs and thicknesses d_{PL} of tBLMs measured with SPR

PL	pH _{max}	R_{max} , $k\Omega$	pK_a^1	d _{PL,} nm
PC	4.0	451.0	2-3	3.68±6%
ePC	3.9	40.2	-	4.10
PE_1	3.4	93.7	2-3	4.59
PE_2	5.9	109.8	8-10	4.59
SM	3.1	343.0	-	3.78
PS	2.8	190.0	1.2	3.57

similar complex dependence on pH (Fig. 2 B). In sharp contrast to R_m and C_m , differences in the thickness (d_m) of the tBLMs measured by SPR [SPR data (Table 2)] are not significant (±10%), agree well with literature values [1] and do not change versus pH (Fig. 3S). The d_m s of PE and ePC show somewhat larger values which can be attributed to the angle of acyl chains with respect to the PL layer [2], i.e., PC = ~17°, PE \approx 0°. Also, the PE tBLMs, formed at pH 4.09, may contribute to a larger PL thickness.

Our resistance and capacitance data for PC are in good agreement with previous data [17], which showed \approx 30 fold decrease in resistivity from pH 5 to 9 and a \approx 4% increase in capacitance. The surge in resistance with R_m from pH 10 to pH 4.0 is the result of protonation and a decrease in the charge of the PL phosphate groups. This is strongly supported by the fact that DOTAP tBLMs, which do not have a phosphate group, do not show a maximum at pH 4.0 (Fig. 7S). Phosphate protonation decreases the surface potential [1,37] of the PC tBLMs, which results in (a) a decrease in the concentration of Na⁺ near the tBLM surface and inside the head groups [37-38], and (b) an increase in the density of the PC hydrocarbon chains; thus, giving rise to the increased resistance of the membrane. In the Ref. [17] the increase in tBLM resistance is attributed to the "existing toroidal pores" model. The size of the pores decreases when lowering the pH from 9 to 5 leading to increase in resistance [17]. Taking into consideration this model and a decrease in concentration of Na⁺ near the PL surface [39] it might be expected that membrane resistance at pHs < 4 would increase or level off due to the positive charge of the choline group. This is not the case. As can be seen in Fig. 2A, the resistance decreases significantly at pHs below the maxima for all tBLMs. The existence of a R_m maximum can most likely be attributed to an increase in concentration of hydronium ions (H₃O⁺) at the lower pHs. The concentration of H_3O^+ at pH 7 is very small (0.1 μ M), but at pH 2 is 20 mM and comparable with the concentration of Na⁺ in the buffer. Furthermore, our data is in accord with the fact that the membrane permeability coefficient of H₃O⁺ is at least 6 orders of magnitude larger than that for sodium ions [5]. It is well known [1] that the first two carbons of the *sn*-2 chain are parallel to the PL membrane plane and the carbonyl oxygen in this chain is available for hydrogen bonding as suggested from molecular dynamics (MD) simulations [19] at lower pHs. MD simulations [18] also show that, at low pHs, H₃O⁺ ions are concentrated at/near this carbonyl oxygen facilitating H₃O⁺ translocation through the membrane. These data may be relevant to earlier theoretical discussions suggesting hydrogen-bonded chains of water extending across the bilayer that promote the H₃O⁺ transfer through the membrane [5,40-42].

The importance of the carbonyl oxygens for the permeability of ions is further evidenced in the data for ePC [43] (Fig. 2 A) that has a phosphate group but lacks the ester functionality (Fig. 1). The ePC tBLMs have a resistance maximum ~10 times smaller than the PC tBLMs despite previous conclusions that the ePC lipids can attain a more densely packed, more rigid bilayers than the diester PC bilayers [43–44]. Significantly, our SPR data shows that the ePC tBLMs are thicker than those for PC (Table 2), in agreement with

the above statement. Large differences are also seen in the capacitance data for these two tBLMs (Fig. 2 B). While the capacitance for the PC tBLMs is in very good agreement with earlier results [17,27], the capacitance for the ePC tBLMs is very different and shows a significant increase from lower to higher pHs (>2 times) in comparison to the increase for the PC tBLMs (~4%). From Eq. (1) [1], one would predict lower capacitance for the ePC tBLMs relative to the PC tBLMs since the thickness (*d*) and the rigidity of ePC bilayers are larger.

$$C = \varepsilon_0 \cdot \varepsilon \cdot A/d \tag{1}$$

where ε_0 is the permittivity of free space, ε is dielectric constant of PL membranes and A is the area of the working electrode.

Using our capacitance data and assuming $\varepsilon = 2.2$, [38] d = 2.6 nm for the PC tBLMs at pH 7.5. This number is significantly lower that the d_m measured by SPR (3.68 nm, Table 2) because it is assumed ϵ = 2.2 reflects only the thickness of the hydrophobic part of the PC [42]. The value d = 2.6 is also smaller than previously reported [45], due to the lower ratio of tethering molecules in the tBLMs [20:80 (tether:BME), compared with 30:70 [45]). Using ε = 2.2 in Eq. (1) to calculate the thickness for the ePC tBLMs we will get an unrealistically small d. By SPR, d = 4.1 (Table 2), suggesting that the dielectric constant of the ePC tBLM is very different from 2.2. Furthermore, it was suggested [2] that the dipole potential created by the carbonyl oxygens in the esters of the PC are responsible for the preferred conductance of sodium ions over chloride ions. The absence of carbonyl oxygens in ePC can be expected to result in an increase in the permeability of chloride ions, which, in turn, would lead to the much smaller resistance of ePC versus PC. These results suggest that the nature of the head groups exhibit significant gating properties for ions through membrane bilayers in the comparison with the gating properties of hydrocarbon chains in total bilayer resistance.

Thus, for all the PLs, the consistent feature of resistance increases from pH 10 to the $R_{\rm max}$ s for the tBLMs at pHs near 3–4 is attributed to the depletion of sodium ions in the PLs head groups due to decreasing the charge of the phosphate groups as one lowers the pH. The resistance decreases from pH 3–4 to 2 is the result of an increase of hydronium ion concentration that form hydrogen bonds with the oxygen atoms (ether or ester) inside the head groups and may cross the membrane with the help of a hydrogen bonding net, as discussed theoretically earlier.

The PS tBLMs (Fig. 1) exhibit a maximum R_m at the lowest pH 2.8 (Table 2) that is less than half the maximum R_m for the PC tBLMs. These tBLMs contain the PL possessing the lowest pK_a value of 1.2, due to the acidity of the phosphate [1] and the carboxyl group. From pH 2 to 10 the capacitance of the PS tBLMs steadily and significantly increases (about 6 times) as compared to the PC tBLMs (4%). Since SPR measurements (Fig. 3S) showed no significant changes in the amount of the material at the surface for the PS tBLMs over this pH range, the dramatic changes in the capacitance most likely reflect changes in dielectric constant ε of the PS tBLM head groups as a function of pH. The dielectric constant [1,37] of membranes depends on the microstructure and the polarizability of the lipid composition. Polarizability is a function of charges, concentration of ions, water in the bilayer, and hydrogen bonds [1]. The increasing negative charge induces preferential interaction with Na⁺ ions [46] of the PS head group at high pHs, due to the presence of the carboxyl group and the possibility of stronger hydrogen bonds [5] at lower pHs. This results in microstructural changes in the lipid layer more complex than that expected in the head group of PC. Our data for the PS and PC tBLMs provide evidence that the terminal groups of the phospholipids (in PS case serine group) and microstructural changes in head groups of the lipids play an important gating role in permeability of ions through the membrane.

SM, on the other hand, differs from PC, not in the head groups but in the acyl chains on the side of the phosphate group closer to the bilayer center (Fig. 1). Whereas PC consists of two vicinal ester linkages to a glycerol moiety, this PL exhibits the ceramides structural features, i.e., lacking a glycerol segment and adding one amide linkage, and a simple hydroxyl group β to the phosphate. As a result, SM bilayers can be expected to more readily form intra- and inter-molecular PL hydrogen bonds [47]. In the membrane, the SM alkyl segments are oriented normal to the bilayer surface [48]. The SM tBLMs show a maximum R_m at pH 3.1, closer to that for the PS tBLMs than the PC tBLMs (Fig. 2 A). The SM tBLMs exhibit a significantly higher capacitance (~2.5 times Fig. 2 B) than PC with a maximum C_m around pH 6. However, despite a much larger capacitance, the resistivity of the SM tBLMs is quite high in comparison with PS (as well as PE), and only about 25% less than PC at its maximum R_m.

The most interesting changes in resistivity and capacitance as a function of pH are for the PE tBLMs, which exhibit two maxima, at pH 3.4 and at 5.9. We hypothesize that the pH 3.4 maximum is attributed to the changes in the ionic character of the phosphate group, as is the case for all the PLs. The R_m at 5.9 is sharp, which is unusual for a pH dependent response, and is larger than the R_m at 3.4. Moreover, the PE tBLMs exhibit a capacitance minimum at pH 5.9 (Fig. 2 B). The capacitance below this pH is essentially the same as for the PC tBLMs, but increases sharply around 7 with irreversible disintegration of the tBLM above pH 8 (SPR shows a reduction in the signal suggesting that some PEs are removed from the surface (data not shown)). We speculate that at this pH the PE tBLM attempts to change curvature of the membrane and as result distorts the planar character of the tBLM. The sharp R_m maximum and capacitance minimum at 5.9 occurs at a value close to an expected isoelectric point (pI) for PE (p $K_a \sim 3$ and 8-9 [5] for the phosphate and the amine groups, respectively), the greatest concentration of electrically neutral molecules, which, in turn, may lead to a decreased surface potential as well as the formation of intramolecular hydrogen bonding [5]. At the higher pHs, the concentration of the protonated amines decrease and the PE molecules are subject to the repulsive negative charge of the phosphate reducing the number intermolecular hydrogen bonds [5] that stabilize the membrane bilayer in spite of previously data (X-ray crystallographic) showing that the amine can form two different types of intermolecular hydrogen bonds [5].

The bilayer structural considerations for the PE tBLMs are supported by comparison with the PG tBLMs (Fig. 8S). Like the PE tBLMS, the PG tBLMs exhibit a large capacitance change at ~ 7 but do not disintegrate at pH ≥ 8 . When the pH is changed back to 7.5, its electrical characteristics almost completely restore (data not shown). SPR data do not show removal of material from the surface before and after change of the pH. To confirm this we conducted NR measurements on PG tBLM that also show no changes in the tBLM hydrophobic thickness versus pH (Table 3; Table 1S; Figs. 9S-13S) of a magnitude that would account for the electrical measurements. The NR measurements do show increased undulation (rms roughness) of the tBLM bilayer at pH 2 and 9, suggesting an increased flexibility that is likely related to the $\sim 10\%$ decrease in

Table 3Neutron reflectometry measurements of the effect of pH on the hydrophobic thickness and rms roughness of PG tBLM at different pHs.

pН	Thickness, nm	RMS roughness, nm
pH 2	$2.725^{+0.016}_{-0.056}$	$0.408^{+0.016}_{-0.019}$
pH 4	$3.089^{+0.010}_{-0.057}$	$0.240^{+0.029}_{-0.026}$
pH 7	$3.067^{+0.008}_{-0.051}$	$0.287^{+0.022}_{-0.027}$
pH 9	$2.623^{+0.013}_{-0.030}$	$0.476^{+0.012}_{-0.017}$

thickness observed at these pH values. The vicinal OH groups in the PG molecules can be expected to sustain an intermolecular hydrogen bond most likely due to a reduction of water-hydroxyl groups interactions with the increase in [Na⁺], as has been suggested earlier [37-38], forming bilayer-stabilizing framework, essentially independent of the pH. Together the PE and PG tBLM data show that the amine group of the PE head group, protonated to the NH₃ ionic state, contributes significantly to the stability of the membrane, largely through charge-charge interactions. When the amine group is not protonated at higher pHs these interactions are reduced and, if the PE bilayers cannot change curvature, the planar membrane disintegrates. The role of the charge of the amine and phosphate groups is further supported by experiments with divalent ions like Ca²⁺ (Fig. 14S). When calcium chloride is added to the PE tBLMs, at pH 6.2 ($[NH_3^+] \gg [NH_2]$), the resistance of the membrane increases 20-fold.

Our data thus support models [1.5] which attribute the gating properties of the membrane to an the interplay between hydrophobic, electrostatic and hydrogen bond forces between the phospholipid molecules of the membrane. pH modulates repulsive/attractive electrostatic forces that, in turn, may change the lateral interactions and structure of the hydrophobic chains of the membrane and reduce or increase the extent of intermolecular hydrogen bonding between the PLs. Taking into consideration that all PLs in this study: 1) have a maximum in resistance, 2) have the same size and composition of acyl chains and, 3) as shown in SPR and NR measurements, have relatively small differences in the tBLM thickness, it's plausible to assume that the gating properties of membranes depend predominately on the nature of the building blocks of PL head group: the ester oxygens, glycerol or ceramides structural features, phosphate groups and terminal groups (serine, choline, amines, hydroxyls). The pH affects the surface electrical potential generated by the PL head group by attracting or repelling ions (Na⁺ or H₃O⁺) and water molecules into the membrane, which, in turn, result in changes in the electrical properties of the

Real cell membranes are composed of mixtures of different types of lipid molecules [2]. Moreover, the composition of bilayers may be asymmetrical, i.e. in plasma membranes, the outer leaflet may consist of mainly one type of lipid, such as PC, SM and Chol, while the inner leaflet consists of other lipids, such as PE, PS, and/or small amounts of signaling PLs such as phosphatidylinositol (PI) [2].

3.2. Model of the plasma membrane outer leaflet

Fig. 3 shows the dependence of the electrical properties of tBLMs composed of PL mixtures known to reflect the compositions of natural plasma membranes versus pH. Although overall the maximum R_ms and C_ms that are observed are close to those observed in Fig. 2, i.e., near pH 4, there are clearly significant differences in the R_ms magnitudes, with large increases in R_m when Chol is in the mixture. It is noteworthy that the dependence of PC/Chol tBLM at pHs > 7 is very close to pure PC tBLM. Cholesterol is known to modulate PL interactions in the membrane [49] in the hydrophobic core of the membrane, largely through void filling inside of the hydrophobic chains, leading to membrane thickening, increased PL packing density, and membrane rigidity [1,49–50]. In addition, the hydroxy group of cholesterol can form hydrogen bonds with the sn-2 acyl chain ester carbonyl oxygens of the PC [1] thus modifying the hydrogen bonding interactions between PLs. Our data (Fig. 3), showing significantly higher resistance (x 1.6) and decreased capacitance in comparison to the PC tBLM (Fig. 3 B) for the PC/Chol tBLMs is in complete accord with these cholesterol-induced structural considerations.

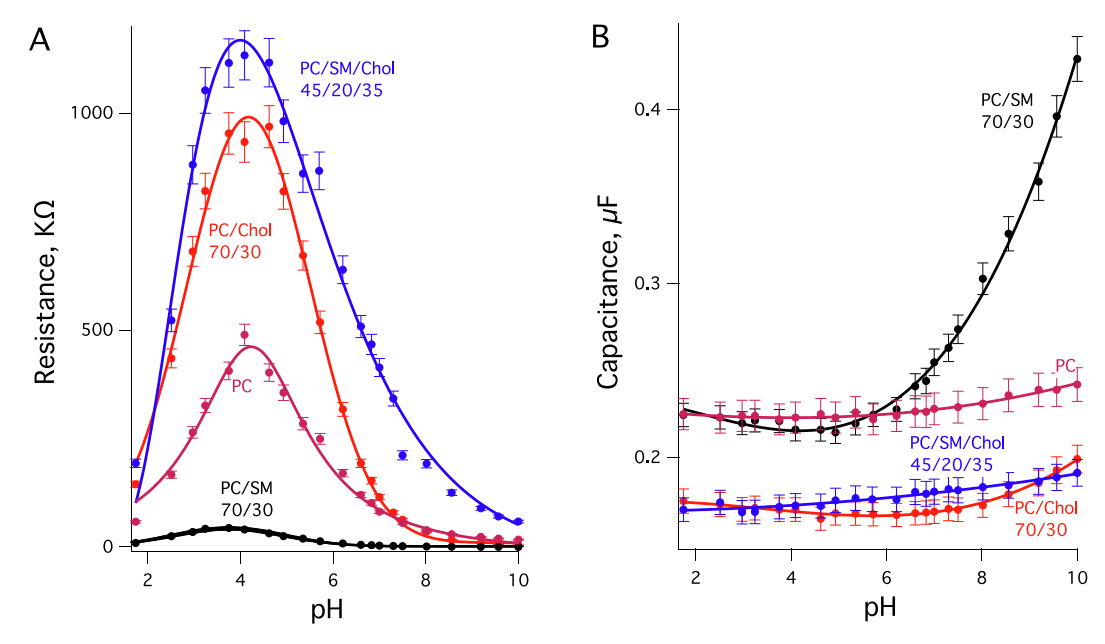


Fig. 3. Dependence on pH of (A) resistance and (B) capacitance of outer leaflet model membrane compositions. tBLMs prepared using mixtures of PLs. Error bars were estimated from the covariance matrix derived from the optimization of the circuit equivalent model (Fig. 1S) to 51 impedance data points using a Levenberg Marquardt algorithm. The purple line, marked PC, is the same as in Fig. 2 and shown here for comparison. Numbers are the ratios of PLs in the mixture. (For interpretation of the references to colour in this figure legend, the reader is referred to the web version of this article.)

In contrast, the PC/SM mixture shows a destabilizing effect on the tBLMs (Fig. 3). Mixing SM with PC significantly reduces the membrane resistance ($\sim \! \times \! 10$) and dramatically increases the capacitance ($\geq \! \times \! 3$ at pHs ≥ 6), compared to the single component PC or SM tBLMs (Fig. 2). It is known [51] that SM in PL mixtures may induce phase separations, promote the formation of negative curvature, make bilayers permeable to small and large solutes, promote flip-flopping of lipids between the leaflets, and induce coupling between membrane leaflets [52] through interdigitation of the SM aliphatic chains. Any of these effects may result in the resistance decreases and capacitance increases observed in our mixed SM/PC tBLMs.

The triple mixture of PC/SM/Chol tBLMs that mimics the outer-leaflet of plasma cell membranes shows an increase in maximum R_m and a decrease in C_m compared with the PC/Chol tBLMs. The addition of SM to the PC/Chol mixture also increases the width of the pH dependence curve and results in steeper resistance changes between pH 4 and 10 when compared with the PC only and PC/Chol tBLMs. Capacitance dependence on pH for the triple mixture is similar to PC/Chol, but is approximately linear, increasing slightly (~5–6%, a bit larger than for the PC only tBLMs) from lower to higher pHs. Overall, the interactions of PC, SM and Chol in mixtures are extremely complex [51,53–54] and greatly depend on the lipid ratios, affecting electrostatic, the hydrophobic and hydrogen bond interactions [47].

3.3. Model of inner leaflet of the membrane

The dependence of tBLM R_ms made with known inner leaflet compositions (Fig. 4) of plasma cells differ markedly from the tBLMs representing outer leaflet compositions. Of the binary tBLMs indicated in Fig. 4, the PE/PS tBLMs exhibit the largest resistance change (>40×) versus pH suggesting that interactions between the PE amine/ammonium groups and the PS carboxyl/carboxylate groups contribute strongly to the gating properties of these tBLMs. Three additional features are noteworthy. 1) The resistance values from pH 7 to 10 for the PE/PS tBLMs are almost the same as for pure PC (Fig. 2A) and PC/PE tBLMs (Fig. 4). 2) Although the PE/PS

tBLMs contained 70% PE, no clear $R_{\rm m}$ maximum was detected at pH 5.9 as was observed for the pure PE tBLMs. 3) The $R_{\rm m}$ maximum is at pH 2.8 similar to that for the pure PS tBLM (Fig. 1). Lastly, the capacitance of the PE/PS tBLMs is below the capacitance of the PC/Chol tBLMs (Fig. 4B) and is the lowest of all the tBLMs measured in this study.

Although the maximum $R_m s$ of the PS and PS/Chol tBLMs (Fig. 2&4A) are essentially the same, the magnitude of the PS/Chol tBLMs R_m is twice as large as that of the PS tBLMs and the decrease, with increase of pH, is more gradual when compared with pure PS tBLMs, which essentially did not change from pH 5 to 10 (Fig. 2).

The PC/PE tBLM has an $R_{\rm m}$ dependence similar to that of pure PC, with a maximum shift toward pH 5. The maximum value of $R_{\rm m}$ is approximately the same as for PC, but the dependence is a little bit broader. The shift of the resistance maximum toward a high pH is most likely the result of the interplay of maxima for PE at pH 5.9 and phosphates of PE and PC at pH 4 and relative concentrations of these PLs in the mixture.

The PE/Chol tBLMs have a pH dependence of R_m with two maxima at pH 4.5 and 5.9 (Fig. 4A). The magnitude of the resistance at the maximal R_m is larger than for the PC/Chol tBLMs (Fig. 2) (1.7×) as is the capacitance (~2× larger). In comparison to pure PE tBLMs that disintegrate above pH 8, Chol provides a strong stabilization effect for the PE membrane.

For the model of inner membrane PL mixtures, changes in the C_ms versus pH (Fig. 4B) are significantly smaller than the single component tBLMs (Fig. 2B), as well as for the outer membrane tBLM models (Fig. 3B), and are in between the capacitance values of pure PC and the PC/Chol tBLMs.

Fig. 5 shows the data for tBLMs composed of triple mixtures of PLs and Chol and one quadruple PLs/Chol mixture. The PE/PS/Chol and the PE/PS/Chol/PC tBLMs mimic compositions and ratios of inner leaflet lipids. Fig. 5A (blue line) also shows for comparison data for PC/SM/Chol tBLMs (This is the same curve as in Fig. 3A) that models the outer leaflets of plasma membranes [2].

The pH dependence of the PE/PS/Chol tBLMs (red line Fig. 5) exhibits a sharp, pronounced maximum at pH 5.9 corresponding to the amine group of PE, and a broader maxima at pH 3.5–4, which

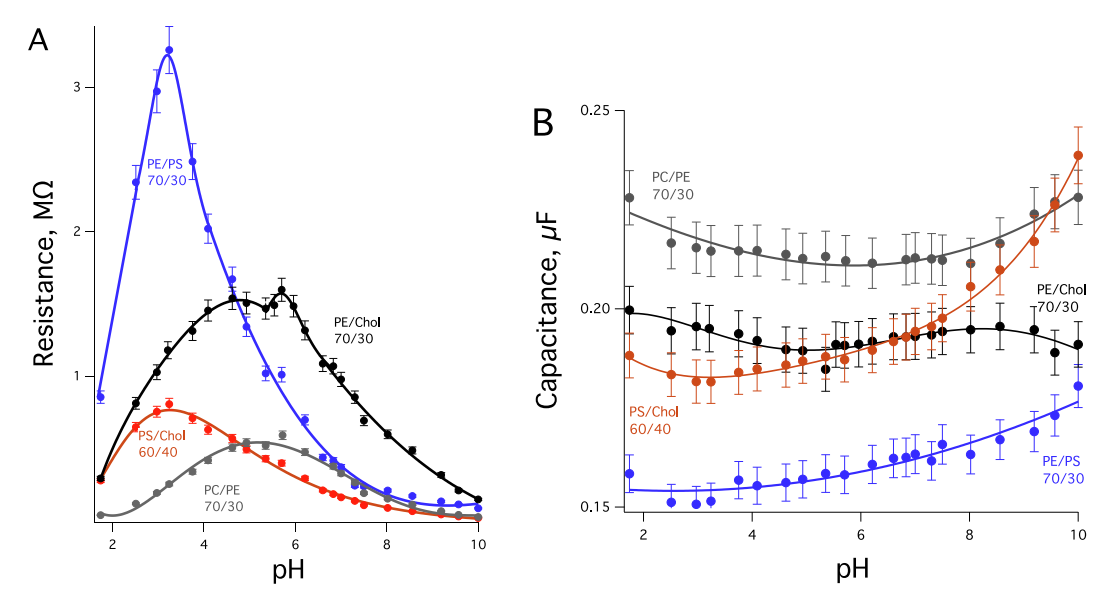


Fig. 4. Dependence on pH of the (A) resistance and (B) capacitance of binary mixtures of PLs from the plasma membrane inner leaflet. Error bars were estimated from the covariance matrix derived from the optimization of the circuit equivalent model (Fig. 1S) to 51 impedance data points using a Levenberg Marquardt algorithm. Numbers are the ratios of PLs in the mixture.

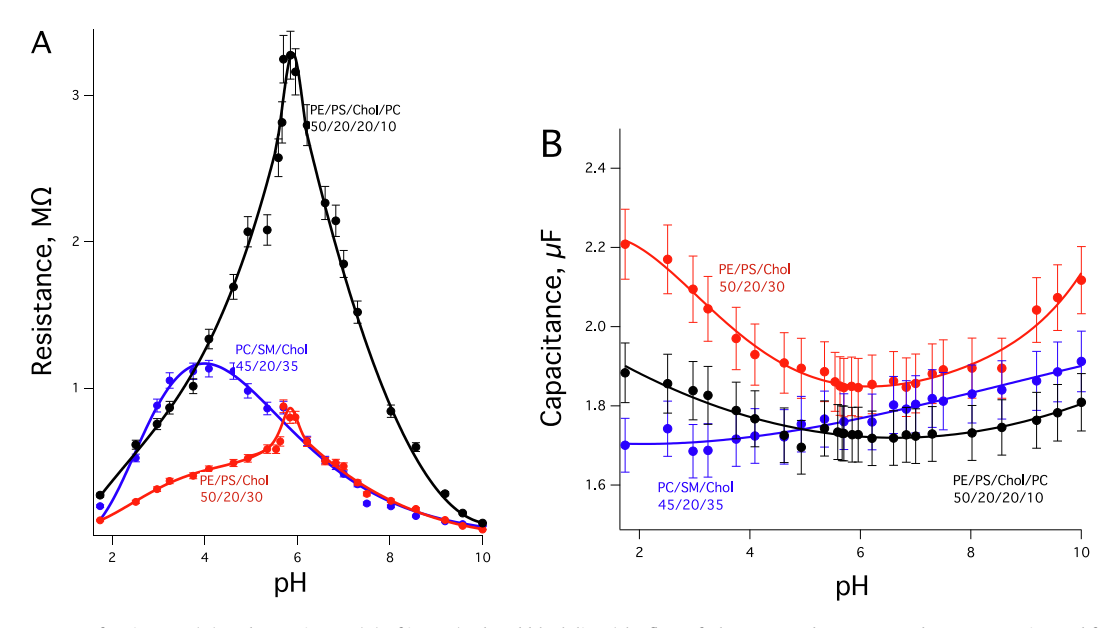


Fig. 5. Dependences on pH of resistance (A) and capacitance (B) of inner (red and black lines) leaflets of plasma membranes. Error bars were estimated from the covariance matrix derived from the optimization of the circuit equivalent model (Fig. 1S) to 51 impedance data points using a Levenberg Marquardt algorithm. Outer leaflet model (blue line PC/SM/Chol) is the same as in Fig. 4 and shown here for comparison. (For interpretation of the references to colour in this figure legend, the reader is referred to the web version of this article.)

appears as a shoulder in the lower pH (pH < 6) part of the curve, attributed to deprotonation of the phosphate groups of the PLs.

Surprisingly, despite the fact that the ratio of PE/PS in the triple mixture did not change significantly in comparison with binary mixture tBLMs (2.5 (Fig. 5 A red line) and 2.3 (Fig. 4 A light blue line)) PS phospholipids influence on the electrical properties of the triple PLs membrane containing Chol is significantly ($3\times$) diminished in comparison with a binary mixture of PE/PS. This suggests that Chol also plays an important role in fine tuning interactions in the head groups of the phospholipids in the inner leaflet of membranes.

Dependences of R_m and C_m on pH for a PE/PS/Chol tBLM and the tBLM model of the outer membrane (red and blue lines correspon-

dently in Fig. 5 A) at the pH range above 6 are approximately the same, however at lower pHs (3–4), the tBLM model of the outer membrane has a resistance more than 3 times larger. Capacitance for the triple PE/PS/Chol mixture has a broad minimum around pH 6 (Fig. 5 B).

To produce a four-component inner membrane model, we mixed PE/PS/Chol/PC, by adding 10% PC to the PE/PS/Chol tBLMs, reducing the Chol by 10% (Fig. 5, black curve). This relatively small change in the tBLM composition dramatically changed the resistance dependence on pH. The resistance increase at maximum R_m was four times the magnitude compared to the ternary tBLMs (Fig. 5A red line) and is comparable with the maximum R_m of the PE/PS tBLMs (Fig. 4A light blue line). Notably, the maximum

R_m for the four component mixture is at pH 6, very close to that found for the single component PE tBLMs (Fig. 2 A, green curve), the PE/Chol tBLMs and the PE/PS/Chol tBLMs (Fig. 4A, black curve and Fig. 5, red curve). For the inner membrane, the slope of change of the resistance at the physiological pHs (6 to 8) is the largest in comparison to all measured tBLMs and differs significantly from the model of the outer membrane (Fig. 5 A, blue line). This may be correlated with important role of PE as a key regulator of membrane fluidity in eukaryotic cells [55].

Comparison of the changes for the inner leaflet model compositions with the outer leaflet model compositions is also informative. Most notably here is that the outer membrane models (Fig. 3 A and Fig. 5, blue line) have the maximum $R_{\rm m}$ = 1.2M Ω at pH 3.5 in contrast to $R_{\rm m}$ = 3.2 M Ω at pH 6 for tBLM of inner membrane (Fig. 5 black line). The inner and outer leaflet models appear to have remarkable similar resistance values from pH 2 to 4 (Fig. 5, compare black and blue curves). From these comparisons, it is clear that the resistance properties of the inner and outer leaflets may vary in dramatically different ways with pH.

Capacitance data for the inner and outer model compositions (e.g., Fig. 5 B, black and blue lines) do not differ significantly. The outer membrane model (PC/SM/Chol tBLMs) exhibits an almost linear change with increasing pH whereas the four-component inner membrane model has a small minimum around 6. The two capacitance values cross at pH 4.9.

The above observations indicate that very small changes in concentration or composition of the PLs in the inner and outer membranes lead to dramatic changes in the properties of the cell membranes. This strongly suggests that when studying interactions of biomolecules with biomimetic membranes these effects must be taken into account.

4. Conclusions

Our work complements and extends recent reports [17–19] on the pH dependence of the permeability of ions through the phospholipid membranes. We demonstrate dramatic effects of pH and lipid composition on the electrical properties of membrane models of the inner and outer leaflets of the plasma membrane over a wide pH range. Lipid compositions varied from individual lipid components to more complex plasma membrane-mimicking mixtures. To emphasize the influence of the building blocks of phospholipids—ester oxygens, glycerol, phosphate and terminal head groups—we kept the aliphatic part of all phospholipids identical.

The resistance of the model membranes reports on the permeability of the membrane to ions. All model membranes, whether composed of single phospholipid species or mixtures, are observed to have resistance maxima at pH values near the pK_a values of the phosphate group, such that these maxima correlate with protonation of the phosphate group. At high pH, the phosphate is negatively charged, resulting in an increase of [Na[±]] in the head groups and smaller membrane resistances. At pH values close to the pK_a , the phosphate is more protonated, the sodium ion concentration is depleted, and the resistance increases. At pH values below the pK_a , the resistance decreases again, due to the increase in hydronium ion concentration and the increase in permeability of these ions, through hydrogen bonding interactions between H₃O[±] and the phosphate and/or carbonyl oxygens of the acyl chains. Single component PE, membranes have additional sharp maxima at pH 5.9 that corresponds to the pI of PE. The resistance values and positions of the R_m maxima, as well as the capacitances of the membranes that contain mixtures of phospholipids differ significantly from single component membranes. Resistance data show the importance of cholesterol in the mixtures, which not only influences the structure of the phospholipids' aliphatic chains, but

also fine tunes the head group interactions. The most dramatic changes with membrane composition are seen in the models of inner membranes that contain PE. The presence of PE in these membranes induces the shift of maximum $R_{\rm m}$ to pH 6. By contrast, the models of the outer leaflet of the membranes have maximum resistance at pH 3—a dramatic difference between the inner and outer leaflets of the membrane.

The membrane capacitance depends both on the membrane thickness and its average dielectric constant. SPR and neutron experimental data show only minor changes in the tBLM thickness over this extensive pH range and agree with previous studies for all compositions. The membrane capacitance, however, does not correlate in a straightforward way with the SPR and NR thicknesses. We thus conclude that our data reflect structural changes in the head groups of the phospholipid molecules and changes in the concentration of salt and hydronium ions due to the collective influences of hydrophobic, electrostatic and hydrogen bond interactions of the lipid molecules.

Taken together, the data reported in this manuscript strongly suggest that electrical properties of the membranes cannot be explained only by changes in the density of the aliphatic chains of the membranes. Changes in charge/hydrogen bonding of the head groups of PLs from pH 2 to pH 10 controls the concentration and permeability of ions through the head groups and the membrane as a whole. Further surface plasmon, electrochemical impedance, and neutron reflectometry studies are underway to understand the influence of concentration of sodium, potassium and divalent ions on pH-dependent membrane electrical properties.

Funding Sources

This research received support in part from the National Science Foundation under grant No. 1714164. Neutron reflectometry data analysis used the Extreme Science and Engineering Discovery Environment (XSEDE), which is supported by National Science Foundation grant number *ACI*-1053575. Specifically, it used the Bridges system, which is supported by NSF award number *ACI*-1445606, at the Pittsburgh Supercomputing Center (PSC).

CRediT authorship contribution statement

Vitalii I. Silin: Conceptualization, Methodology, Investigation, Data curation, Writing - original draft, Writing - review & editing, Formal analysis, Visualization. **David P. Hoogerheide:** Investigation, Data curation, Validation, Formal analysis, Writing - review & editing, Visualization.

Declaration of Competing Interest

The authors declare that they have no known competing financial interests or personal relationships that could have appeared to influence the work reported in this paper.

Acknowledgment

Authors are grateful to Dr. David Vanderah, emeritus Fellow of Institute for Bioscience and Biotechnology Research, for valuable discussions and thorough reading and editing of the manuscript, Dr. John Marino at National Institute of Standards and Technology (NIST) and Dr. David Worcester at NIST Center for Neutron Research for support and useful suggestions to improve the manuscript. We acknowledge the National Institute of Standards and Technology, US Department of Commerce, for providing the neutron research facilities used in this work. The investigations utilized nanofabrication facilities at NIST, Gaithersburg, MD USA.

Certain commercial materials, equipment, and instruments are identified in this work to describe the experimental procedure as completely as possible. In no case does such an identification imply a recommendation or endorsement by NIST, nor does it imply that the materials, equipment, or instrument identified are necessarily the best available for the purpose.

Appendix A. Supplementary material

Experimental procedures, EIS and SPR data, phospholipid structure and additional data for data comparison are included in the supporting information.

The Supporting Information is available free of charge on the ACS Publications website.

Supplementary data to this article can be found online at https://doi.org/10.1016/j.jcis.2021.03.016.

References

- [1] R.B. Gennis, Biomembranes Molecular structure and function, Springer Science +Business Media, LLC: New York, 1989, p 236.
- [2] G. van Meer, D.R. Voelker, G.W. Feigenson, Membrane lipids: where they are and how they behave, Nat. Rev. Mol. Cell Biol. 9 (2) (2008) 112–124.
- [3] U. Coskun, M. Grzybek, D. Drechsel, K. Simons, Regulation of human EGF receptor by lipids, Proc. Natl. Acad. Sci. U S A 108 (22) (2011) 9044–9048.
- [4] B. Brugger, Lipidomics: analysis of the lipid composition of cells and subcellular organelles by electrospray ionization mass spectrometry, Annu. Rev. Biochem. 83 (2014) 79–98.
- [5] J.M. Boggs, Lipid intermolecular hydrogen bonding: influence on structural organization and membrane function, Biochim. Biophys. Acta 906 (3) (1987) 353-404
- [6] N.B.F. Duzgunes, Membrane fusion in fertilization cellular transport, and viral infection, Curr. Topics Membr. Transport 32 (1988) (0070-2161), 384.
- [7] X. Ou, Y. Liu, X. Lei, P. Li, D. Mi, L. Ren, L. Guo, R. Guo, T. Chen, J. Hu, Z. Xiang, Z. Mu, X. Chen, J. Chen, K. Hu, Q. Jin, J. Wang, Z. Qian, Characterization of spike glycoprotein of SARS-CoV-2 on virus entry and its immune cross-reactivity with SARS-CoV, Nat. Commun. 11 (1) (2020) 1620.
- [8] D.L. Esposito, J.B. Nguyen, D.C. DeWitt, E. Rhoades, Y. Modis, Physico-chemical requirements and kinetics of membrane fusion of flavivirus-like particles, J. Gen Virol. 96 (Pt 7) (2015) 1702–1711.
- [9] J. Llopis, J.M. McCaffery, A. Miyawaki, M.G. Farquhar, R.Y. Tsien, Measurement of cytosolic, mitochondrial, and Golgi pH in single living cells with green fluorescent proteins, Proc. Natl. Acad. Sci. U S A 95 (12) (1998) 6803–6808.
- [10] F.R. Maxfield, Role of endosomes and lysosomes in human disease, Cold Spring Harb. Perspect. Biol. 6 (5) (2014) a016931.
- [11] W.N. Konings, S.V. Albers, S. Koning, A.J. Driessen, The cell membrane plays a crucial role in survival of bacteria and archaea in extreme environments, Antonie Van Leeuwenhoek 81 (1–4) (2002) 61–72.
- [12] C. Baker-Austin, M. Dopson, Life in acid: pH homeostasis in acidophiles, Trends Microbiol. 15 (4) (2007) 165–171.
- [13] E. Padan, E. Bibi, M. Ito, T.A. Krulwich, Alkaline pH homeostasis in bacteria: new insights, Biochim. Biophys. Acta 1717 (2) (2005) 67–88.
- [14] M.I. Angelova, A.F. Bitbol, M. Seigneuret, G. Staneva, A. Kodama, Y. Sakuma, T. Kawakatsu, M. Imai, N. Puff, pH sensing by lipids in membranes: The fundamentals of pH-driven migration, polarization and deformations of lipid bilayer assemblies, Biochim. Biophys. Acta Biomembr. 1860 (10) (2018) 2042–2063
- [15] M.S. Bretscher, Asymmetrical lipid bilayer structure for biological membranes, Nat. New Biol. 236 (61) (1972) 11–12.
- Nat. New Biol. 236 (61) (1972) 11–12.
 [16] S.M. Baumler, A.M. McHale, G.J. Blanchard, Surface charge and overlayer pH influence the dynamics of supported phospholipid films, J. Electroanal. Chem. (Lausanne) 812 (2018) 159–165.
- [17] C.G. Cranfield, T. Berry, S.A. Holt, K.R. Hossain, A.P. Le Brun, S. Carne, H. Al Khamici, H. Coster, S.M. Valenzuela, B. Cornell, Evidence of the key role of H30 (+) in phospholipid membrane morphology, Langmuir 32 (41) (2016) 10725–10734.
- [18] E. Deplazes, D. Poger, B. Cornell, C.G. Cranfield, The effect of hydronium ions on the structure of phospholipid membranes, Phys. Chem. Chem. Phys. 20 (1) (2017) 357–366.
- [19] E. Deplazes, D. Poger, B. Cornell, C.G. Cranfield, The effect of H3O(+) on the membrane morphology and hydrogen bonding of a phospholipid bilayer, Biophys. Rev. 10 (5) (2018) 1371–1376.
- [20] K. Lahdesmaki, O.H. Ollila, A. Koivuniemi, P.T. Kovanen, M.T. Hyvonen, Membrane simulations mimicking acidic pH reveal increased thickness and negative curvature in a bilayer consisting of lysophosphatidylcholines and free fatty acids, Biochim. Biophys. Acta 1798 (5) (2010) 938–946.
- [21] M. Naumowicz, Z.A. Figaszewski, The effect of pH on the electrical capacitance of phosphatidylcholine-phosphatidylserine system in bilayer lipid membrane, J. Membr. Biol. 247 (4) (2014) 361–369.

- [22] A.D. Petelska, Z.A. Figaszewski, Effect of pH on the interfacial tension of bilayer lipid membrane formed from phosphatidylcholine or phosphatidylserine, Biochim. Biophys. Acta 1561 (2) (2002) 135–146.
- [23] R. Sandeaux, P. Seta, G. Jeminet, M. Alleaume, C. Gavach, The influence of pH on the conductance of lipid bimolecular membranes in relation to the alkaline ion transport induced by carboxylic carriers grisorixin, alborixin and monensin, Biochim. Biophys. Acta 511 (3) (1978) 499–508.
- [24] Y. Zhou, R.M. Raphael, Solution pH alters mechanical and electrical properties of phosphatidylcholine membranes: relation between interfacial electrostatics, intramembrane potential, and bending elasticity, Biophys. J. 92 (7) (2007) 2451–2462.
- [25] D. Marquardt, B. Geier, G. Pabst, Asymmetric lipid membranes: towards more realistic model systems, Membranes (Basel) 5 (2) (2015) 180–196.
- [26] H. Hauser, M.C. Phillips, M. Stubbs, Ion permeability of phospholipid bilayers, Nature 239 (5371) (1972) 342–344.
- [27] D.J. McGillivray, G. Valincius, D.J. Vanderah, W. Febo-Ayala, J.T. Woodward, F. Heinrich, J.J. Kasianowicz, M. Losche, Molecular-scale structural and functional characterization of sparsely tethered bilayer lipid membranes, Biointerphases 2 (1) (2007) 21–33.
- [28] D.R. Scott, V. Silin, H. Nanda, Reconstitution of functionalized transmembrane domains of receptor proteins into biomimetic membranes, Langmuir 31 (33) (2015) 9115–9124.
- [29] B.A. Cornell, V.L. Braach-Maksvytis, L.G. King, P.D. Osman, B. Raguse, L. Wieczorek, R.J. Pace, A biosensor that uses ion-channel switches, Nature 387 (6633) (1997) 580–583.
- [30] B. Rakovska, T. Ragaliauskas, M. Mickevicius, M. Jankunec, G. Niaura, D.J. Vanderah, G. Valincius, Structure and function of the membrane anchoring self-assembled monolayers, Langmuir 31 (2) (2015) 846–857.
- [31] R. Eells, P. Hoogerheide David, A. Kienzle Paul, M. Lösche, F. Majkrzak Charles, F. Heinrich, 3. Structural investigations of membrane-associated proteins by neutron reflectometry, in: Characterization of Biological MembranesStructure and Dynamics, 2019.
- [32] P. Shekhar, H. Nanda, M. Losche, F. Heinrich, Continuous distribution model for the investigation of complex molecular architectures near interfaces with scattering techniques, J. Appl. Phys. 110 (10) (2011) 102216–10221612.
- [33] N.A. Nystrom, M.J. Levine, R.Z. Roskies, J.R. Scott, Bridges, in: Proceedings of the 2015 XSEDE Conference on Scientific Advancements Enabled by Enhanced Cyberinfrastructure - XSEDE '15, ACM, St. Louis, Missouri, 2015, pp 1–8.
- [34] J. Towns, T. Cockerill, M. Dahan, I. Foster, K. Gaither, A. Grimshaw, V. Hazlewood, S. Lathrop, D. Lifka, G.D. Peterson, R. Roskies, J.R. Scott, N. Wilkens-Diehr, XSEDE: accelerating scientific discovery, Comput. Sci. Eng. 16 (5) (2014) 62–74.
- [35] J.A. Vrugt, C.J.F. ter Braak, C.G.H. Diks, B.A. Robinson, J.M. Hyman, D. Higdon, Accelerating Markov chain monte carlo simulation by differential evolution with self-adaptive randomized subspace sampling, Int. J. Nonlin Sci. Num. 10 (3) (2009) 273–290.
- [36] P.A. Kienzle, J. Krycka, N. Patel, C. Metting, I. Sahin, Z. Fu, W. Chen, A. Mont, D. Tighe, Refl1D (Version 0.7.7) [Computer Software], University of Maryland, College Park, MD, 2016.
- [37] E. Gongadze, A. Velikonja, Š. Perutkova, P. Kramar, A. Maček-Lebar, V. Kralj-Iglič, A. Iglič, Ions and water molecules in an electrolyte solution in contact with charged and dipolar surfaces, Electrochim. Acta 126 (2014) 42–60.
- [38] R. Vacha, S.W. Siu, M. Petrov, R.A. Bockmann, J. Barucha-Kraszewska, P. Jurkiewicz, M. Hof, M.L. Berkowitz, P. Jungwirth, Effects of alkali cations and halide anions on the DOPC lipid membrane, J. Phys. Chem. A 113 (26) (2009) 7235–7243.
- [39] J. Kotynska, Z.A. Figaszewski, Adsorption equilibria between liposome membrane formed of phosphatidylcholine and aqueous sodium chloride solution as a function of pH, Biochim. Biophys. Acta 1720 (1–2) (2005) 22–27.
- [40] N. Amdursky, Y. Lin, N. Aho, G. Groenhof, Exploring fast proton transfer events associated with lateral proton diffusion on the surface of membranes, Proc. Natl. Acad. Sci. U S A 116 (7) (2019) 2443–2451.
- [41] D.W. Deamer, Proton permeation of lipid bilayers, J. Bioenerg Biomembr. 19 (5) (1987) 457–479.
- [42] J.F. Nagle, Theory of passive proton conductance in lipid bilayers, J. Bioenergy Biomembr. 19 (5) (1987) 413–426.
- [43] J.M. Dean, I.J. Lodhi, Structural and functional roles of ether lipids, Protein Cell 9 (2) (2018) 196–206.
- [44] J.M. Smaby, A. Hermetter, P.C. Schmid, F. Paltauf, H.L. Brockman, Packing of ether and ester phospholipids in monolayers. Evidence for hydrogen-bonded water at the sn-1 acyl group of phosphatidylcholines, Biochemistry 22 (25) (1983) 5808–5813.
- [45] G. Valincius, T. Meskauskas, F. Ivanauskas, Electrochemical impedance spectroscopy of tethered bilayer membranes, Langmuir 28 (1) (2012) 977– 990
- [46] J. Pan, X. Cheng, L. Monticelli, F.A. Heberle, N. Kucerka, D.P. Tieleman, J. Katsaras, The molecular structure of a phosphatidylserine bilayer determined by scattering and molecular dynamics simulations, Soft Matter. 10 (21) (2014) 3716–3725.
- [47] J.P. Slotte, The importance of hydrogen bonding in sphingomyelin's membrane interactions with co-lipids, Biochim. Biophys. Acta 1858 (2) (2016) 304–310.
- [48] M.F. Renne, A.I. de Kroon, The role of phospholipid molecular species in determining the physical properties of yeast membranes, FEBS Lett. 592 (8) (2018) 1330-1345.
- [49] R.S. Cantor, Lipid composition and the lateral pressure profile in bilayers, Biophys. J. 76 (5) (1999) 2625–2639.

- [50] T. Rog, M. Pasenkiewicz-Gierula, I. Vattulainen, M. Karttunen, Ordering effects of cholesterol and its analogues, Biochim. Biophys. Acta 1788 (1) (2009) 97-
- [51] A. Alonso, F.M. Goni, The physical properties of ceramides in membranes, Annu. Rev. Biophys. 47 (2018) 633–654. [52] T. Rog, A. Orlowski, A. Llorente, T. Skotland, T. Sylvanne, D. Kauhanen, K.
- Ekroos, K. Sandvig, I. Vattulainen, Interdigitation of long-chain sphingomyelin induces coupling of membrane leaflets in a cholesterol dependent manner, Biochim. Biophys. Acta 1858 (2) (2016) 281–288.
- [53] F.M. Goni, A. Alonso, Biophysics of sphingolipids I. Membrane properties of sphingosine, ceramides and other simple sphingolipids, Biochim. Biophys. Acta 1758 (12) (2006) 1902–1921.
- [54] F.M. Goni, A. Alonso, Effects of ceramide and other simple sphingolipids on
- membrane lateral structure, Biochim. Biophys. Acta 1788 (1) (2009) 169–177.

 [55] R. Dawaliby, C. Trubbia, C. Delporte, C. Noyon, J.M. Ruysschaert, P. Van Antwerpen, C. Govaerts, Phosphatidylethanolamine is a key regulator of membrane fluidity in eukaryotic cells, J. Biol. Chem. 291 (7) (2016) 3658-